Trace elements and Pb isotopes in soils and sediments impacted by uranium mining

Alicia Cuvier, Laurent Pourcelot, Anne Probst, Jérôme Prunier, Gaël Le Roux

Trace elements and Pb isotopes in soils and sediments impacted by uranium mining

A. Cuvier [a,b,*], L. Pourcelot [b], A. Probst [a], J. Prunier [c], G. Le Roux [a]

[a] ECOLAB, Université de Toulouse, CNRS, INPT, UPS, Toulouse, France
[b] IRSN/PRP-ENV/SESURE/Laboratoire d'études radioécologiques en milieu continental et marin, BP 1, 13108 Saint Paul Lez Durance Cedex, France
[c] Observatoire Midi-Pyrénées, laboratoire Géosciences Environnement Toulouse, CNRS/IRD/Université Paul Sabatier, 14 avenue Edouard Belin, 31400 Toulouse, France

HIGHLIGHTS

- Contamination of soils is evidenced by a multiproxy approach.
- Enrichment factors highlight a low contamination except for U, S and Ba.
- Pb isotope ratios point out inputs of radiogenic Pb from the mine.
- Radiogenic Pb is mainly in the acid-soluble and the reducible fractions.

GRAPHICAL ABSTRACT

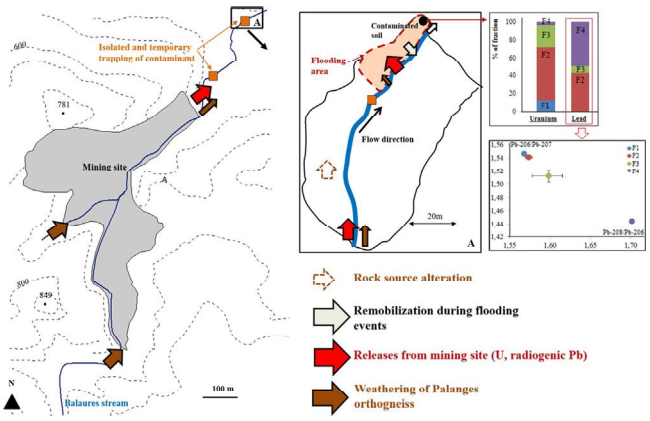

ABSTRACT

The purpose of this study is to evaluate the contamination in As, Ba, Co, Cu, Mn, Ni, Sr, V, Zn and REE, in a high uranium activity (up to 21,000 $Bq \cdot kg^{-1}$) area, downstream of a former uranium mine. Different geochemical proxies like enrichment factor and fractions from a sequential extraction procedure are used to evaluate the level of contamination, the mobility and the availability of the potential contaminants. Pb isotope ratios are determined in the total samples and in the sequential leachates to identify the sources of the contaminants and to determine the mobility of radiogenic Pb in the context of uranium mining.

In spite of the large uranium contamination measured in the soils and the sediments ($EF \gg 40$), trace element contamination is low to moderate ($2 < EF < 5$), except for Ba ($5 < EF < 15$), due to the precipitation of barium sulfate resulting from mining activities. Most of the trace elements are associated with the most mobile fractions of the sediments/soils, implying an enhanced potential availability.

Even if no Pb enrichment is highlighted, the Pb isotopic signature of the contaminated soils is strongly radiogenic. Measurements performed on the sequential leachates reveal inputs of radiogenic Pb in the most mobile fractions of the contaminated soil. Inputs of low-mobile radiogenic Pb from mining activities may also contribute to the Pb signature recorded in the residual phase of the contaminated samples. We demonstrate that Pb isotopes are efficient tools to trace the origin and the mobility of the contaminants in environments affected by uranium mining.

* Corresponding author.
E-mail addresses: alicia.cuvier@hotmail.fr (A. Cuvier), gael.leroux@ensat.fr (G. Le Roux).

1. Introduction

Mining activities contribute to approximately 46% of the total anthropogenic flux of uranium to the environment (Sen and Peucker-Ehrenbrink, 2012). Uranium mining is often associated with environmental releases of non-radioactive contaminants from ore, waste rocks and reagents used in the extraction process. In addition to uranium, Noller (1991) measured a significant increase of Mg, Mn and S (as sulfate ions) from milling process, in the aquatic ecosystem. U, V, Cr, Cd, Ni, Cu, Zn, As, Mo, W and Cd were found to be enriched in soils located on a former uranium ore heap in Germany (Carlsson and Büchel, 2005). Fe, K, U, Zn and lanthanides were enriched in Argentinian topsoils, due to a former open-cast operation uranium mine (Bermudez et al., 2010). As is commonly associated with uranium enrichment in sediments near former uranium mines (Kipp et al., 2009, Larson and Stone, 2011).

Different indices, like the enrichment factor (EF) (Chester and Stoner, 1973, Covelli and Fontolan, 1997), are used to evaluate the degree of contamination. These indices concern only the total concentration and do not provide any indication about the distribution in the different soil phases. If the degree of contamination is low, EF may not be significant, in particular if the material chosen as a reference is not appropriate (N'Guessan et al., 2009, Reimann and de Caritat, 2005). That is why these indices must be coupled with other procedures allowing the determination of the mobility and bioavailability of the contaminants.

Among indicators of contamination, sequential extractions offer a good compromise between information on the distribution of element among the solid fractions/components and the potential risks associated with their mobility or their bioavailability. In the framework of the Standards, Measurements and Testing Program (SMTP), an harmonization of extraction protocols led to a standardized 3-step procedure (Quevauviller et al., 1994, Rauret et al., 1999). This procedure allows the determination of three operationally extractable fractions that can predict the nature and the content of trace elements, potentially released in case of modifications of environmental parameters like pH or redox conditions. Its reproducibility and repeatability were confirmed by various studies (Davidson et al., 1998; Rauret, 1998; Whalley and Grant, 1994). The enhanced BCR sequential extraction protocol has been widely adopted and applied to different media including uranium contamination (Bartosiewicz et al., 2015, Dhoum and Evans, 1998, Howe et al., 2002, Martin et al., 1998, Meca et al., 2012, Smodiš et al., 2012, Štrok and Smodiš, 2013).

In the case of anthropogenic contamination, the origin and the mobility of Pb can be assessed by the measurement of Pb isotopes in sequential leachates (Bäckström et al., 2004, Bacon et al., 2006, Hirner, 1992, Probst et al., 2003, Steinmann and Stille, 1997). Water, soils, sediments or living organisms contaminated by U-ore or U-mining products show specific radiogenic Pb signatures. That is why Pb isotopes are frequently used as potential tracers of U-mining pollution (Bollhöfer and Martin, 2003, Bollhöfer et al., 2006, Frostick et al., 2008, 2011, Kyser et al., 2015, Santos and Tassinari, 2012). However, to our knowledge, no Pb isotope measurement has ever been made on sequential leachates of soil or sediment contaminated by U-ore or U-mining products. Clearly there is a lack of information about the mobility of radiogenic Pb in the context of uranium mining.

This study aims to combine enrichment factor, sequential extractions and Pb isotope ratios in soils and sediments highly contaminated by uranium as a result of past U-mining activities, in order to assess (1) other potential harmful trace element (PHTE) contamination, (2) the mobility of contaminants and (3) their potential source(s).

2. Methods

2.1. Studied site

The Bertholène mine is located in the Palanges forest, within the Palanges orthogneissic massif, an alkali monzogranite, mainly constituted by microclines, quartzs, plagioclase feldspars and micas (biotite and muscovite). Accessory minerals include sphenes, rutiles, apatites, allanites, thorites, zircons, monazites and yttrium phosphates. Uranium ore and associated weathering were described by Schmitt et al. (1984) and Lévêque (1988). The exploitation of the Bertholène uranium ore was performed as underground (1981–1992) and open pit (1983–1995) mines, leading to the production of 744 tons of uranium and 470,000 tons of tailings. The site was equipped with an in-situ uranium ore pre-processing unit, of which functioning is described in Humbert (1986). Since the beginning of the mine operation, effluent waters from mines, tailings dams and barren materials have been collected and neutralized with lime, sodium hydroxide and flocculating agents, before being released into the Balaures stream. A previous gamma spectrometry mapping of the radionuclide distribution has shown strong enrichments in U-decay products, downstream of the mine, in a flooding area frequently submerged by the Balaures stream (see the colorful inset in Fig. 1 and the supplementary material SI-1). Activity of U-238 as high as 21,000 $Bq \cdot kg^{-1}$ has been measured, with strong disequilibrium in the U-238 decay chain (Cuvier et al., 2015). The Balaures stream, flowing through the mining site, is contaminated by the mining activities and has been identified as the main vector of radionuclide transfer.

2.2. Sampling protocols

2.2.1. Soils and sediments

A total of seven soil surface horizons were sampled in the downstream area, using an 8 cm diameter stainless steel corer (Fig. 1). Two sampling points, namely P0 and P3, were located in the non-contaminated areas, on the left and on the right riverbanks of the Balaures stream respectively. Five sampling points, namely P1, P2, P8, P13 and P10 were sampled in the radionuclide accumulation area (see the supplementary material SI-1). All the profiles were 25 cm length except the uncontaminated profile P3 of 35 cm length. At each sampling site, three cores were collected and each core was sampled in sub-sections of 5 cm length all the way along the core. The three corresponding slices were then mixed together, in order to minimize heterogeneity.

1 kg of surface river bottom sediments of the Balaures stream was collected by hand upstream and downstream of the mine. Soil and sediment samples were collected in plastic bag and kept to 4 °C before preparation.

After air-drying the soils and sediments, coarse particles (gravels) and organic debris (roots) were removed. Soil and sediment samples were carefully homogenized, quartered and sieved at 2 mm using nylon sieves. The sieve analyses were performed on the representative aliquots by the Société du Canal de Provence (COFRAC accreditation), according to the standard AFNOR X31 107. Four grain sizes were identified: coarse sand (2 mm–0.2 mm), fine sand (0.2 mm–0.05 mm), silts (0.05 mm–0.002 mm) and clays (<0.002 mm). Trace element and Pb isotopes contents were determined on the <2 mm fraction using aliquots previously crushed with an agate mortar.

2.2.2. Vegetation

Aerial parts of ray-grasses and undifferentiated forage crops (1 m above the soil) were collected in uncontaminated and radionuclide contaminated areas (Fig. 1). Samples were cut using a ceramic knife on a surface covering around 1 m^2. Samples were rinsed with ultrapure H_2O before drying at 40 °C and crushing.

2.3. Sequential extraction procedure

Sequential extractions were performed on the 5–10 cm layer of the selected soils and sediments, according to the revised procedure of Rauret et al. (1999). All reactants were ultrapure grade and supplied by VWR. For each sample, three replicates were performed and the accuracy of the process was confirmed by analyses of CRM BCR-701 (see Supplementary Information SI-2). An internal check was also realized

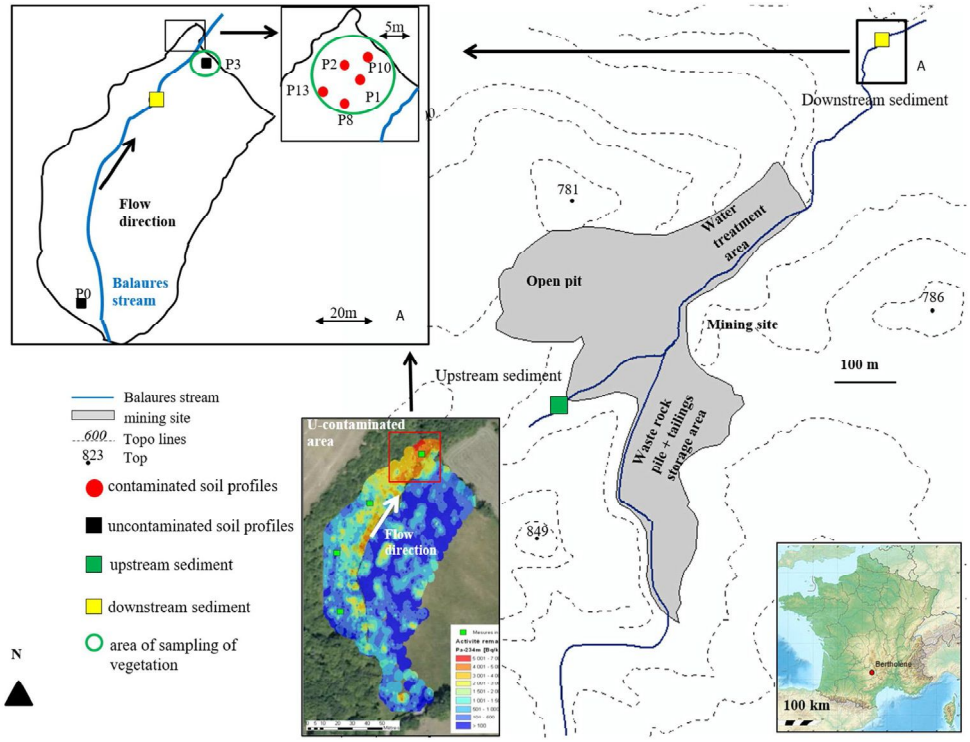

Fig. 1. Location of the former uranium mine of Bertholène, the downstream radionuclide contaminated area and the main sampling points (soils, forage vegetation and sediment). Map of the distribution of the activity of Pa-234m (U-238) is from the study of Cuvier et al. (2015), see supplementary material SI-1 for the magnification of the radionuclide distribution map. (For interpretation of the references to color in this figure, the reader is referred to the web version of this article.)

by comparing the concentration of the target element in the total sample (determined by ALS laboratory (Sevilla, Spain)) and the sum of the four sequential fractions. Most of the percentages of recovery were included between 90% and 110% even if some values were ranged from 80% to 90%, depending on the sample. All procedural blanks were negligible ($<10^{-4}$ mg·kg^{-1}).

2.4. Analytical measurements

2.4.1. Major and trace element analysis

All experiments and analyses performed on the different samples are summarized in Table 1. Trace element concentrations were measured in bulk soils by ALS laboratory. The accuracy of the ICP-MS measurements was checked using a natural river water (SLRS-5) (Yeghicheyan et al., 2013) and a certified lake sediment (SUD-1). The detection limits ranged from 0.01 μg·kg^{-1} to 0.1 μg·kg^{-1} depending on the element.

2.4.2. Determination of ($^{206}Pb/^{207}Pb$) and ($^{208}Pb/^{206}Pb$) isotope ratios in bulk samples, sequential leachates and plant samples

Selected samples were diluted in HNO_3 2% to reach a final total Pb concentration of 500 ng·kg^{-1}. Pb isotope ratios were determined by HR-ICP-MS (Observatoire Midi-Pyrénées, Toulouse, France). Mass bias correction was evaluated using standard-sample bracketing technique, by measurement of NIST SRM 981 (concentration of standard solution = 500 ng·kg^{-1}) after each sample (Krachler et al., 2004).

2.5. Calculations

2.5.1. Statistical tests

All the statistical analyses were realized using STATISTICA 8 software. For the ray-grass and the forage crops data set, assumptions of differences, between the groups growing on the contaminated and the uncontaminated areas, were tested using a parametric *t*-test. Normality of the distribution of the data was assessed using the Shapiro-Wilks test (p-value < 0.05), before each statistical treatment. Homogeneity of variance was assessed using the Levene and the Brown and Forsythe tests. Correlations were evaluated using the parametric Pearson correlation coefficient.

2.5.2. Enrichment factor

EF is defined as the concentration ratio of a considered element to a reference element in a given sample, divided by the same ratio in a reference material (Chester and Stoner, 1973):

$$EF = \frac{\left[\frac{\text{Element}}{\text{Reference element}}\right]_{\text{sample}}}{\left[\frac{\text{Element}}{\text{Reference element}}\right]_{\text{reference material}}}.$$

The earth crust can be chosen as reference material if data are not available. Nevertheless, the use of local background values as reference material is an alternative method more suitable to take into account local background specificity (Blaser et al., 2000; Bourennane et al., 2010; Hernandez et al., 2003). In this study, the local background values were estimated from the deepest layer (25–35 cm) of the reference profile (P3), namely $P3_{25-35}$. The normalization of the trace element concentration of this sample by the upper continental crust (UCC) (Wedepohl, 1995) shows that $P3_{25-35}$ was significantly enriched in U, As, and Pb and depleted in Co, Cu and Ni compared to the UCC. To overcome this potential bias, two EF values were calculated for the contaminated soils, using (1) the deepest layer $P3_{25-35}$ and (2) the UCC as references.

The choice of the reference element depends on some requirements previously defined (Luoma, 1990; N'Guessan et al., 2009). Different lithogenic elements like Al (Windom et al., 1989), Fe (Schiff and Weisberg, 1999), Cs (N'Guessan et al., 2009), Zr (Blaser et al., 2000), Sc (Hernandez et al., 2003) or Ti have been already used. However, Fe, Sc and Cs are mobile in our soil and sediment samples, since their proportions in the residual fraction were 86.7%, 75.8% and 88.3% respectively. The proportions of Al, Ti and Zr in the residual phase, 94.9%, 99.8%

Table 1
List of analyses performed on soils, sediments and plants samples. The reagents, the measuring devices, the measured elements and the location of measurements are also specified (OMP = GET (OMP, Toulouse); ALS = ALS (Sevilla, Spain)). Sequential extraction were performed following the protocol of Rauret et al. (1999).

Target fraction	Extractive reagent	Reagent/sample ratio	Temperature	pH	Time	Analyze	Measured elements	Location
Bulk sample (ALS)	0.250 g of sample + $HClO_4$ + HNO_3 + HF					ICP-AES	Al, Ca, Fe, Mn	ALS
	HCl					Q-ICP-MS	Ba, U, Th, REE, Co, Ni, Zn, As	ALS
	11% HCl						^{206}Pb, ^{207}Pb, ^{208}Pb	
						HR-ICP-MS		OMP
F1: acid-soluble	0.11 M CH_3COOH	40:1	22 ± 2 °C	3 ± 0.2	16 h	ICP-AES	Al, Ca, Fe, Mn	EcoLab
						Q-ICP-MS	Ba, U, Th, REE, Co, Ni, Zn, Cd, As	OMP
							^{206}Pb, ^{207}Pb, ^{208}Pb	
						HR-ICP-MS		OMP
F2: reducible	0.5 M $NH_2OH \cdot HCl$	40:1	22 ± 2 °C	1.5 ± 0.2	16 h	ICP-AES	Al, Ca, Fe, Mn	EcoLab
	0.05 M HNO_3					Q-ICP-MS	Ba, U, Th, REE, Co, Ni, Zn, Cd, As	OMP
							^{206}Pb, ^{207}Pb, ^{208}Pb	
						HR-ICP-MS		OMP
F3: oxidizable	9.79 M H_2O_2	10:1	22 ± 2 °C		1 h	ICP-AES	Al, Ca, Fe, Mn	EcoLab
			85 ± 2 °C		1 h	Q-ICP-MS	Ba, U, Th, REE, Co, Ni, Zn, Cd, As	OMP
	9.79 M H_2O_2	10:1	85 ± 2 °C		1 h		^{206}Pb, ^{207}Pb, ^{208}Pb	
	1 M NH_4Ac	50:1	22 ± 2 °C	2 ± 0.1	16 h	HR-ICP-MS		OMP
F4: residue	Microwave digestion: 0.250 g of dry		200 °C		20 min	ICP-AES	Al, Ca, Fe, Mn	EcoLab
	residue + 14.1 M HNO_3 + 9.85 M		70 °C			Q-ICP-MS	Ba, U, Th, REE, Co, Ni, Zn, Cd, As	OMP
	HCl + HF 40%		120 °C				^{206}Pb, ^{207}Pb, ^{208}Pb	
	H_2O_2 30% v/v + $HClO_4$		100 °C			HR-ICP-MS		OMP
	H_3BrO_4 + 6 M HCl + H_2O MiliQ		150 °C					
	Evaporation		90 °C					
	7.5 N HNO_3							
Plant samples	HNO_3 69%		85 °C		2 days	Q-ICP-MS	Major + trace elements, REE, U/Th	OMP
	8.8 M H_2O_2 + H_2O MiliQ						^{206}Pb, ^{207}Pb, ^{208}Pb	
						HR-ICP-MS		OMP

and 98.9% respectively, indicated that these elements were conservative in soils. However, (1) the Al concentration was higher in the contaminated soils than in the uncontaminated ones (see Supplementary Information SI-3) and (2) Zr showed no significant linear correlation with any studied element. Finally, Ti was selected as reference element (R^2 ranging from 0.24 to 0.92 depending on the element, $p < 0.05$, $n = 20$, see Supplementary Information SI-4). The enrichment factors (EF) were the calculated using UCC (Wedepohl, 1995) and $P3_{25-35}$ as reference materials.

3. Results

3.1. Trace elements contents in soils, sediments and plants

Although no specific guideline values exist for sediments affected by uranium mining activities, Thompson et al. (2005) presented sediment quality guidelines (SQGs) for Al, Cu, Pb, Ni, V and radionuclides released to the aquatic environment during mining or milling of uranium ore. In our study, trace element concentrations are higher in downstream sediment than in the upstream one (Table 2). They are significantly higher than the LEL (Lowest Effect Level, i.e. the concentration that 95% of benthic biota can tolerate) for U, As and Ni but still well below the Severe Effect Level (SEL (weighted) (concentration at which pronounced effects can be expected), respectively 5874, 346 and 484 $mg \cdot kg^{-1}$ (Thompson et al., 2005).

The concentrations of U, Ba, V, As, Co, Ni and Zn and Rare Earth Elements (REE) like La, Gd and Yb are significantly higher in the contaminated soil samples than in the uncontaminated ones (Table 2).

Significantly higher concentrations (parametric *t*-test, $p < 0.05$) of Mn, Ba, Ni, Zn, La and U concentrations are noticed in the ray-grasses and the undifferentiated forage crops growing on the radionuclide contaminated area (Table 2). On the contrary, the concentration of arsenic is lower in the contaminated samples than in the uncontaminated ones.

3.2. Distribution of trace elements in soils and sediments

In this study, F1 is the acid-soluble fraction, F2 and F3 the reducible and the oxidizable ones and finally F4 is the residue. Thus, trace elements can be divided into five groups, depending on their distribution among the different fractions (Fig. 2 and Table 3):

- **Group A** is constituted by **Cu** and **Ni**, which have a similar distribution, depending on the nature of the sample. The percentages of the acid-soluble and the oxidizable fractions of the two elements are higher in contaminated samples than in the uncontaminated ones.
- **Group B** includes **As**, **Ba** and **V**. The proportion of the residual fraction of these elements varies from 65% to 94%, whatever the nature of the samples or the presence of contamination. Zn was associated to this group since in the percentage of the residual fraction varies from 67% to 89% in the two soils and in the upstream sediment. On the contrary, the percentage of Zn in the acid-soluble fraction is higher in the downstream sediment than in the other samples.
- **Group C** includes Mn and Co. The percentages of the acid-soluble and the reducible fractions of the two elements are the largest in all samples. Moreover, the reducible fraction of the two elements is higher in the contaminated samples than in the uncontaminated ones.
- **Group D** includes **Pb**, **La**, **Gd** and **Yb**. The distribution of these elements are dominated by the reducible and the residual fractions. The percentages of the REE in the reducible and in the oxidizable fractions of the contaminated samples are higher than in the uncontaminated ones. The acid-soluble fraction of the downstream sediment has the highest concentration in these elements. The percentage of Pb is higher in the reducible and in the residual fractions of both soils, i.e. around 50% each one, but the percentage of the reducible fraction is higher in the downstream sediment than in the upstream one, i.e. 53% and 13% respectively.
- **Group E** includes **U** only. This element has an intermediate behavior between group C and group D, depending on the considered samples.

Table 2
Concentration in major and trace elements measured in bulk samples (soil, sediments and vegetation). Values are in % for Al, Ca, Mg, P, Fe, Ti, Mn, S and Ba and in $mg \cdot kg^{-1}$ for the others elements. $P3_{25-35}$ is the deepest soil layer of the profile P3 (see Fig. 1).

Nature	Location	pH	OM	Clay	Al[a]	Fe[c]	Ti	Mn[b]	S[b]	Ba[b]	U*,[b]	V[a]	As[b]	Co[a]	Cu	Ni[b]	Pb	Zn[a]	La[a]	Gd[b]	Yb[a]
			%								$mg \cdot kg^{-1}$										
Sediment	UPS n = 1	5.6	2.1	2.6	4.4	0.3	0.1	0.01	0.02	0.09	4.4	4	0.9	1	2	1	18	11	21	5.2	3.4
	DWS n = 1	7	4.1	4.6	4.3	1.8	0.2	0.27	0.10	0.14	273	40	32.3	19	18	31	31	122	38	8.8	4.1
Soil	UNC n = 4	6.4 ± 0.3	4.5 ± 1	17.1 ± 1.4	4.93 ± 0.31	1.91 ± 0.35	0.3 ± 0.1	0.08 ± 0.01	0.06 ± 0.02	0.08 ± 0.05	11 ± 3	59 ± 10	27 ± 5	9 ± 4	46 ± 43	16 ± 6	49 ± 8	107 ± 57	35 ± 2	5.2 ± 0.3	3.5 ± 0.3
	C n = 10	6.6 ± 0.1	7.6 ± 2.6	13.8 ± 2.9	6.8 ± 0.9	2.2 ± 0.4	0.3 ± 0.0	0.22 ± 0.03	0.20 ± 0.02	0.65 ± 0.12	1005 ± 370	92 ± 27	62 ± 13	29 ± 8	43 ± 14	44 ± 10	54 ± 6	179 ± 35	76 ± 20	24 ± 8	10 ± 3
	REF $P3_{25-35}$ n = 1	5.7	2	17.2	5.2	1.8	3	0.07	0.04	0.05	8.7	54	23	7	10	12	46	72	39	5.7	3.8
Vegeta-tion	UNC n = 3				0.002 ± 0.001	0.003 ± 0.000	_	0.004 ± 0.000	_	0.002 ± 0.000	0.002 ± 0.000	_	0.034 ± 0.005	_	1.9 ± 0.6	0.5 ± 0.1	0.11 ± 0.01	18 ± 3	0.030 ± 0.006	_	_
	C n = 3				0.003 ± 0.002	0.005 ± 0.001	_	0.007 ± 0.001	_	0.004 ± 0.000	0.4 ± 0.2	_	0.020 ± 0.005	_	1.9 ± 0.5	1.5 ± 0.3	0.14 ± 0.08	25 ± 1	0.040 ± 0.007	_	_
LEL (weighted) (Thompson et al., 2005)											101	35	9.8		22	21	38				

UPS = upstream, DWS = downstream, UNC = uncontaminated area, C = contaminated area, _ = under the detection level of Q-ICP-MS.
t-Test, n = 14.
[a] $p < 0.05$.
[b] $p < 0.001$.
[c] Only for vegetation (n = 12).

The percentage of uranium is higher in the acid-soluble and the reducible fractions of the contaminated samples than in the reducible and in the residual fractions of the uncontaminated ones.

3.3. Determination of Pb isotope ratios

3.3.1. In soils, sediments and plants

The isotopic background ($^{208}Pb/^{206}Pb = 2.09$ and $^{206}Pb/^{207}Pb = 1.204$) is determined as the average ratios of bottom samples (0.9–1 m depth) from a peat core (around 1 m depth) sampled upstream of the mine outside mining influence (Cuvier, 2015). Uncontaminated soil shows Pb signature close to the isotopic background with $^{208}Pb/^{206}Pb$ ratios of 2.060 ± 0.002 and $^{206}Pb/^{207}Pb$ ratios of 1.20 ± 0.001. A slight enrichment in ^{206}Pb and ^{207}Pb appears in the downstream sediment compared to the geochemical background. On the contrary, the contaminated soils are characterized by values of 1.520 ± 0.001 and 1.620 ± 0.002 for the $^{206}Pb/^{207}Pb$ and $^{208}Pb/^{206}Pb$ ratios respectively. The $^{208}Pb/^{206}Pb$ ratio indicates that enrichment concerns mainly the radiogenic Pb isotopes from the U-238 decay chain and not from the Th-232 decay chain.

The Pb isotope ratios of the vegetation are 1.16 ± 0.003 and 2.1 ± 0.003 in the uncontaminated area and 1.18 ± 0.009 and 2.07 ± 0.003 in the radionuclide contaminated area, for the $^{206}Pb/^{207}Pb$ and $^{208}Pb/^{207}Pb$ ratios, respectively.

3.3.2. In sequential leachates

Pb isotope ratios are measured in the sequential leachates (Table 3). The low difference (<3%) between the sum of the Pb isotopic ratio of the different extracted fractions, weighted by their Pb content, and the ratio of the total samples, validates the sequential extraction and the measurement procedures.

In the uncontaminated soil, the Pb isotope ratios of the residue (F4) are similar to those of the total soil (Fig. 3). In the contaminated soil, the most radiogenic ratios are measured in the acid-soluble (F1) and the reducible (F2) fractions. The Pb isotope ratios of the residue (F4) differ from the previous fractions even if the values remain strongly radiogenic compared to the uncontaminated samples.

In the downstream sediment, the Pb isotope ratios of the three first fractions (F1, F2 and F3) are significantly different from the upstream one, but not particularly radiogenic. The residual fractions (F4) of the upstream sediment and one replicate of the downstream one show radiogenic Pb isotope ratios. The Pb isotopes ratios of the residual phase (F4) of the downstream sediment are highly heterogeneous.

4. Discussion

4.1. Evaluation of the contamination degree

EF values ranging between 0.5 and 2 are considered in the range of natural variability, whereas ratios above 2 indicate enrichments corresponding to anthropogenic inputs (Ettler et al., 2006, Hernandez et al., 2003). Significant enrichments in U, Ba, S, Gd, Mn, Sr, Cu, As, Yb, Zn and La are found in the contaminated soils, whatever the reference material used (Fig. 4 and Supplementary Information SI-5). Co and Ni are concerned only if $P3_{25-35}$ is used as reference material, due to the depletion of the geochemical background in those elements, compared to the UCC, as evidenced in soils from non-mining areas (Hernandez et al., 2003) (see Supplementary Information SI-5). V and Pb are not significantly enriched (EF < 2). Both EFs of U ($P3_{25-35}$ or UCC ≫ 40) underline the extreme degree of contamination of this element in the topsoil and in the sediment. An anthropic contribution (5 < EF < 20) is highlighted for Ba, S, Gd and Mn, depending on the nature of the contaminated samples (soil or sediment). The background concentrations in As, Gd, Pb and Yb are higher than the UCC ones, as already observed for As in stream sediments from the Midi-Pyrénées region (N'Guessan et al., 2009). Thus, the EF UCC (Ti) values are probably overestimated. Considering the local reference background, low contamination (2 ≤ EF ≤ 5) is expected for those elements.

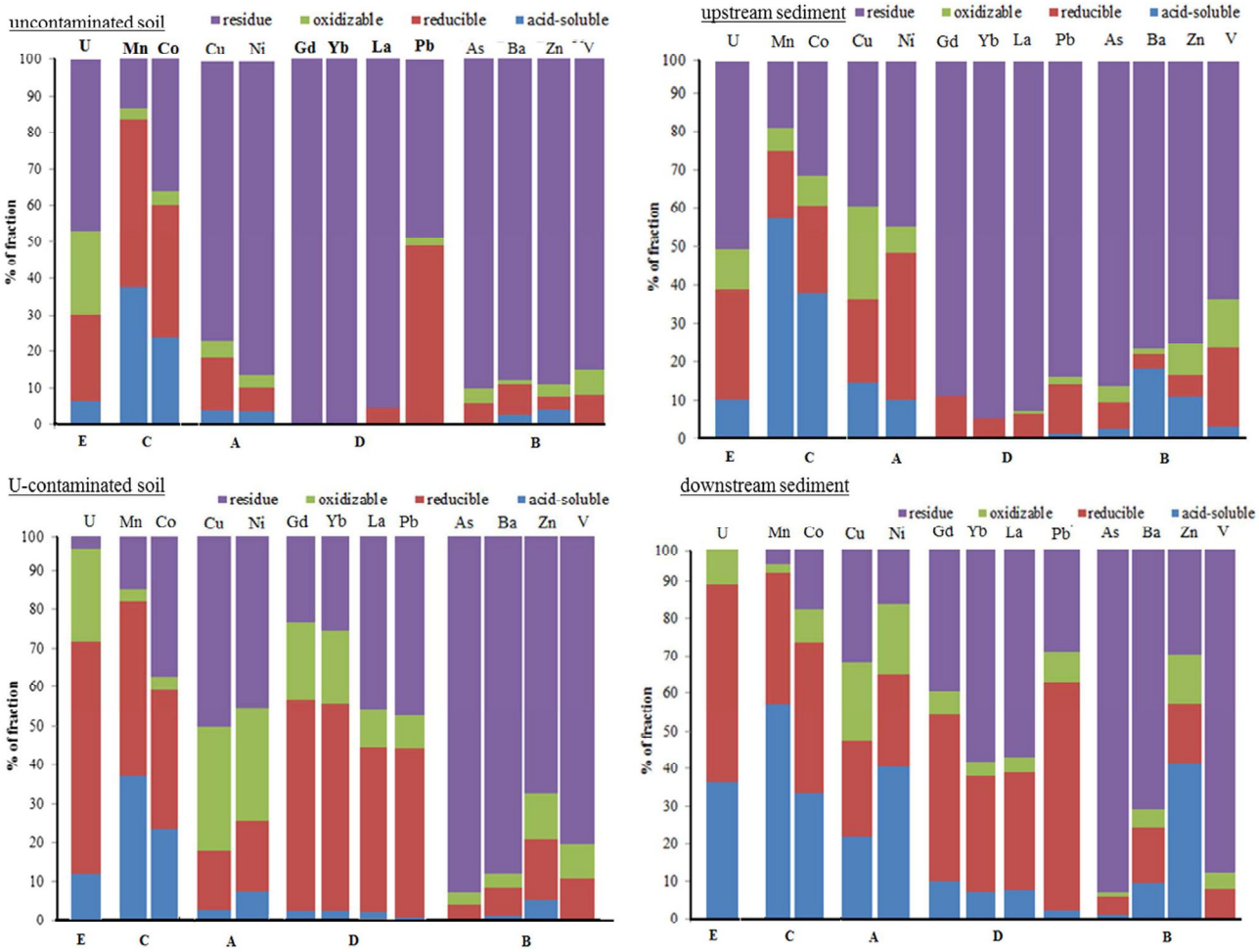

Fig. 2. Distribution of trace elements in uncontaminated and contaminated samples given by sequential extraction. E = group of uranium, C = group including Mn and Co, A = group including Cu and Ni, D = group including Gd, Yb, La and Pb and B = group including the least mobile elements as Ba, V, As and Zn.

4.2. Location of the contaminants in the affected soils and sediments

Correlations existing between enrichment factors and soil parameters can provide information on the location of the contaminants among the different soil grain size or soil phases and help to identify parameters controlling the deposition and the accumulation. In this way, on our samples, a relationship was tentatively performed between the EF calculated for the <2 mm fraction and the fine fraction content.

Significant correlations ($r = 0.79–0.93$, $R^2 = 0.63–0.86$, $p < 0.05$, $n = 9$) are found between the EFs of V, As, Cu, U and REE and the percentage of the fine fraction (<0.05 mm, i.e. % of clays + % of silts) in the contaminated samples. Co EF and Ni EF are moderately correlated with the percentage of silts only ($r = 0.74–0.76$, $R^2 = 0.55–0.57$, $p < 0.05$, $n = 8$). Fe and Al total concentrations are strongly correlated with the enrichment factor of REE, U, V, Cu and As ($r = 0.77–0.99$, $R^2 = 0.59–0.97$, $p < 0.01$, $n = 10$), but moderately correlated with the EFs of Co and Ni and Pb ($r = 0.67–0.87$, $R^2 = 0.45–0.75$, $p < 0.05$, $n = 10$). EF Zn is moderately correlated with the EF of Mn only ($r = 0.78$, $R^2 = 0.61$, $p < 0.01$, $n = 10$). These statements support the idea that metal enrichments are essentially located in the fine fraction (<0.05 mm), as previously found for the radionuclides of the U-decay chains (Cuvier et al., 2015). It could be explained either by inputs of fine particles (clays and/or Al-, Fe–Mn-oxides) carrying those elements and/or by inputs of those elements as colloidal or dissolve forms following by adsorption, complexation, co-precipitation or ion-exchange reactions on fine particles in the contaminated soil.

4.3. Changes of the partitioning of trace elements in the contaminated samples

The enrichment factor is calculated from the total concentration and does not reflect the availability of the contaminants. Even if the As concentration of the downstream sediment is around 3 times higher than the LEL, the sequential extraction indicates that this element is mainly located in the residual fraction, thus under a non-available form. The calculation of the enrichment factor (EF) is not sensitive enough to confirm the contamination in Co and Ni in the contaminated soils. The sequential extractions highlight clear changes in the distribution of Ni and Co, involving an increase of the potential availability of both elements from uncontaminated to contaminated soils. These results are consistent with the study of Skipperud et al. (2013), showing that Ni is mainly found as low molecular mass species, i.e. mobile and potentially available, in stream waters contaminated by tailing material from uranium heap leaching. Finally, anthropogenic origin can be also expected for Ni and Co, explaining the modification of the distribution of the two elements in the soils and sediments.

Despite the calculation of EFs of Ba and As confirming the enrichment of both elements in the contaminated samples, their relative distribution show only a slight increase of the residual fraction (Table 3). In the case of barium, it can be associated with the increase of strongly insoluble barium sulfate minerals. The little increase of the arsenic concentration in the residual fraction could be explained by a strong retention of this element inside the clay fraction or in the crystalline Fe-

Table 3
Concentration in $mg \cdot kg^{-1}$ (based on the weight of dry sample) and average distribution of each element (expressed in % of the total and normalized to 100) measured in each leachate. R % is the percentage of recovery calculated from total concentrations. Pb isotope ratios measured in each sequential leachate of the uncontaminated and the contaminated samples are also indicated. For the downstream sediment, values of the residual fraction of each replicates are given.

Element		As		Ba		Co		Cu		Gd		La		Mn	
Sample	Fraction	$mg \cdot kg^{-1}$	%	$mg \cdot kg^{-1}$	%	$mg \cdot kg^{-1}$	%	$mg \cdot kg^{-1}$	%	$mg \cdot kg^{-1}$	%	$mg \cdot kg^{-1}$	%	$mg \cdot kg^{-1}$	%
Upstream sediment	F1	0.03 ± 0.00	2.1	151 ± 4	17.8	0.2 ± 0.0	39	0.3 ± 0.0	14.4	_	_	0.2 ± 0.0	0.8	36 ± 1	58.2
n = 3 replicates	F2	0.1 ± 0.0	6.9	32 ± 4	3.8	0.1 ± 0.0	23.2	0.5 ± 0.0	21.9	0.6 ± 0.0	10.8	1.5 ± 0.1	6.2	11 ± 2	17.9
	F3	0.1 ± 0.0	4.3	11 ± 1	1.3	0.03 ± 0.00	7.7	0.5 ± 0.0	24	_	_	0.3 ± 0.0	1.1	3.6 ± 0.3	5.6
	F4	1.2 ± 0.3	86.7	3.4 ± 0.4	77.1	0.1 ± 0.0	30.6	0.9 ± 0.1	39.6	5.1 ± 1.6	86.4	25 ± 10	91.9	9.8 ± 2	17.9
	R %	**98 ± 19**		**99 ± 2**		**82 ± 4**		**90 ± 9**		**110 ± 31**		**104 ± 39**		**80 ± 3**	
Downstream sediment	F1	0.4 ± 0.0	1.1	117 ± 8	9.1	6.3 ± 0.8	33.1	3.9 ± 0.3	21.8	1 ± 0.1	9.9	3.2 ± 0.3	8	1549 ± 143	57.2
n = 3 replicates	F2	1.5 ± 0.1	4.6	200 ± 4	15.1	7.7 ± 0.3	40.6	4.6 ± 0.3	25.4	4.4 ± 0.3	44.5	13 ± 1	31.7	942 ± 14	34.8
	F3	0.4 ± 0.1	1.3	55 ± 4	4.4	1.6 ± 0.1	8.6	3.7 ± 0.9	20.7	0.6 ± 0.1	6	1.6 ± 0.4	4	59 ± 3	2.2
	F4	30 ± 4	93.1	947 ± 225	71.4	1.3 ± 0.2	17.7	8.3 ± 2.1	32	4 ± 0.6	39.5	23 ± 3	56.3	55 ± 13	5.9
	R %	**101 ± 11**		**97 ± 17**		**89 ± 7**		**108 ± 4**		**109 ± 6**		**106 ± 9**		**96 ± 5**	
Uncontaminated soil P3	F1	0.2 ± 0.0	0.9	19 ± 1	3.9	1.6 ± 0.1	23.7	0.5 ± 0.0	4.3	_	_	0.1 ± 0.0	_	275 ± 14	37.3
Layer 5–10 cm	F2	1.5 ± 0.0	6.2	41 ± 4	8	2.4 ± 0.1	36.3	1.6 ± 0.1	14.4	_	_	1.7 ± 0.0	5.5	334 ± 20	45.3
n = 3 replicates	F3	0.9 ± 0.0	3.8	6.3 ± 0.2	1.3	0.2 ± 0.0	3.4	0.5 ± 0.0	4.9	_	_	0.3 ± 0.0	_	23 ± 1	3.2
	F4	22 ± 3	89.1	441 ± 23	86.8	2.4 ± 0.2	36.6	8.3 ± 0.4	76.5	4.2 ± 0.7	100	31 ± 3	93.4	104 ± 11	14.2
	R %	**88 ± 5**		**96 ± 4**		**94 ± 3**		**108 ± 4**		**104 ± 14**		**95 ± 10**		**106 ± 3**	
Contaminated soil P2	F1	0.3 ± 0.0	0.2	101 ± 2	1.3	3.3 ± 0.1	10.1	1.9 ± 0.0	2.7	0.9 ± 0.0	2.2	2 ± 0.0	1.8	509 ± 14	26.4
Layer 5–10 cm	F2	3.6 ± 0.1	3.5	540 ± 24	7	18 ± 1	53.2	11 ± 1	15.2	22 ± 1	55.2	47 ± 3	42.8	1243 ± 58	63.6
n = 3 replicates	F3	3.5 ± 0.5	3.5	278 ± 12	3.7	3.1 ± 0.2	9.5	23 ± 2	32	8.1 ± 0.7	20	10 ± 1	9.7	48 ± 3	2.5
	F4	94 ± 2	92.8	6706 ± 105	88	8.9 ± 0.2	27.2	36 ± 2	50.1	9.1 ± 0.2	22.6	49 ± 1	45.7	142 ± 0	7.4
	R %	**104 ± 2**		**100 ± 2**		**91 ± 1**		**102 ± 0**		**104 ± 6**		**99 ± 2**		**93 ± 0**	

		Ni		Pb		U		V		Yb		Zn			
Sample	Fraction	$mg \cdot kg^{-1}$	%	$mg \cdot kg^{-1}$	%	$mg \cdot kg^{-1}$	%	$mg \cdot kg^{-1}$	%	$mg \cdot kg^{-1}$	%	$mg \cdot kg^{-1}$	%	$^{206}Pb/^{207}Pb$	$^{208}Pb/^{206}Pb$
Upstream sediment	F1	0.2 ± 0.0	9.8	0.4 ± 0.0	2	0.3 ± 0.0	10.9	0.1 ± 0.0	2.9	_	_	1.6 ± 0.2	10.5	1193 ± 0001	2074 ± 0002
n = 3 replicates	F2	0.7 ± 0.0	38.3	2.4 ± 0.2	13	0.9 ± 0.1	29	0.7 ± 0.0	20.5	0.1 ± 0.0	5.7	0.9 ± 0.1	5.8	1191 ± 0001	2076 ± 0001
	F3	0.1 ± 0.0	6.7	0.4 ± 0.0	2.1	0.3 ± 0.0	10.4	0.4 ± 0.0	12.3	_	_	1.2 ± 0.1	7.9	1197 ± 0002	2070 ± 0003
	F4	0.7 ± 0.1	45.1	16 ± 1	82.9	1.6 ± 0.4	49.8	2.3 ± 0.4	64.3	2.1 ± 0.3	92.38	12 ± 3	75.7	1432 ± 0004	1722 ± 0004
	R %	**86 ± 9**		**104 ± 4**		**85 ± 3**		**82 ± 12**		**110 ± 16**		**91 ± 20**		n.m.	n.m.
Downstream sediment	F1	13 ± 1	39.6	0.7 ± 0.0	1.9	108 ± 9	35.6	0.1 ± 0.0	0.2	0.3 ± 0.0	7.5	51 ± 4	39	1226 ± 0001	2009 ± 0001
	F2	7.6 ± 0.3	23.9	19 ± 2	52.7	156 ± 12	51.4	3.1 ± 0.1	7.6	1.3 ± 0.1	30.9	19 ± 1	14.8	1220 ± 0005	2020 ± 0009
n = 3 replicates	F3	5.9 ± 0.3	18.5	2.5 ± 0.7	7	31 ± 2	9.9	1.8 ± 1	4.5	0.2 ± 0.0	3.9	16 ± 2	12.6	1222 ± 0016	2015 ± 0036
	F4	5.7 ± 0.4	17.9	14 ± 3	38.4	9 ± 4	3.2	33 ± 1	87.8	2 ± 0.4	57.7	44 ± 8	33.6	1454 (n = 1)	1681 (n = 1)
	R %	**102 ± 6**		**107 ± 2**		**111 ± 9**		**95 ± 4**		**90 ± 9**		**106 ± 9**		1.237 (n = 2)	2.004 (n = 2)
														1.226 ± 0.001**	**2.013 ± 0.002****
Uncontaminated soil P3	F1	0.4 ± 0.0	3.7	0.6 ± 0.1	1.3	0.6 ± 0.0	7.5	0.1 ± 0.0	0.3	_	_	4.1 ± 0.2	5.2	1183 ± 0006	2076 ± 0004
	F2	0.8 ± 0.1	6.4	21 ± 1	48.2	2 ± 0.2	23.6	3.9 ± 0.0	9	_	_	2.7 ± 0.1	3.4	1191 ± 0001	2072 ± 0001
Layer 5–10 cm	F3	0.4 ± 0.0	3.5	0.9 ± 0.1	2.2	1.9 ± 0.2	22.3	2.9 ± 0.1	6.6	_	_	2.7 ± 0.1	3.5	1193 ± 0001	2069 ± 0001
n = 3 replicates	F4	10 ± 1	86.3	21 ± 2	48.3	3.9 ± 0.4	46.5	37 ± 6	84.1	3.1 ± 0.4	100	71 ± 5	89.1	1205 ± 0004	2059 ± 0005
	R %	**100 ± 7**		**106 ± 4**		**91 ± 9**		**85 ± 12**		**92 ± 1**		**97 ± 5**		**1.20 ± 0.001****	**2.060 ± 0.002****
Contaminated soil P2	F1	4.2 ± 0.1	7.3	0.3 ± 0.0	0.5	204 ± 4	12.1	0.1 ± 0.0	0.1	0.3 ± 0.0	2.1	11 ± 1	4.6	1547 ± 0002	1568 ± 0001
	F2	10.7 ± 0.5	18.1	27 ± 1	44.3	1023 ± 33	60.1	15 ± 0	10.7	7.8 ± 0.3	54	43 ± 1	16	1541 ± 0003	1574 ± 0004
Layer 5–10 cm	F3	16.6 ± 0.4	28.9	5.0 ± 0.2	8.3	408 ± 11	24.2	12 ± 6	8.9	2.8 ± 0.2	19	28 ± 2	11.9	1512 ± 0009	1599 ± 0021
n = 3 replicates	F4	27.9 ± 0.9	45.7	28 ± 0	46.9	62 ± 26	3.6	111 ± 9	80.4	3.5 ± 0.0	26	162 ± 34	67.3	1445 ± 0001	1702 ± 0001
	R %*	**100 ± 1**		**98 ± 1**		**99 ± 4**		**94 ± 2**		**94 ± 3**		**104 ± 1**		**1.520 ± 0.001****	**1.620 ± 0.002****

F1 = acid-soluble, F2 = reducible, F3 = oxidizable and F4 = residue.
_ = under the detection level of Q-ICP-MS.
n.m. = not measured.
* R % = (F1 + F2 + F3 + F4) / bulk * 100.
** Lead isotope ratios of total sample.

oxides, only poorly dissolved during the second step of the sequential procedure.

The trace metal contamination is associated with an increase of the REE content, in the following order Gd > Yb > La. According to Rao et al. (2010), the REE are mainly distributed between the reducible and the residual fractions of the contaminated samples. More generally, the operationally-defined reducible fraction appears as a major trace metal carrier of U and REE in the contaminated samples (Fig. 2).

4.4. Calculation of the transfer factors in vegetation

In order to assess the bio-availability of the contaminants, calculation of the transfer factors was performed on the ray-grasses and the undifferentiated forage crops sampled in the contaminated and the uncontaminated area, using the concentration of the acid-soluble fraction (expressed in $mg \cdot kg^{-1}$ of dry soil) of the 5–10 cm layer (Fig. 5). The TF values of Al, Mn, Fe, As, Pb and U are similar between both locations, but the TF values of Mg, Ca, Ni, Cu, Co, Ba and La are lower in ray-grasses sampled on the contaminated area. However, these results must be interpreted with caution since (1) the major and trace element fraction really available for plant uptake is not defined using this sequential extraction procedure, (2) the acid-soluble fraction of the upper soil layer (0–5 cm) was not measured and (3) the indiscriminate collection of different grasses limits the value of this data for interpretation. Additionally, the major and trace elements concentrations in roots were not determined, whereas they can be the main storage organs of trace

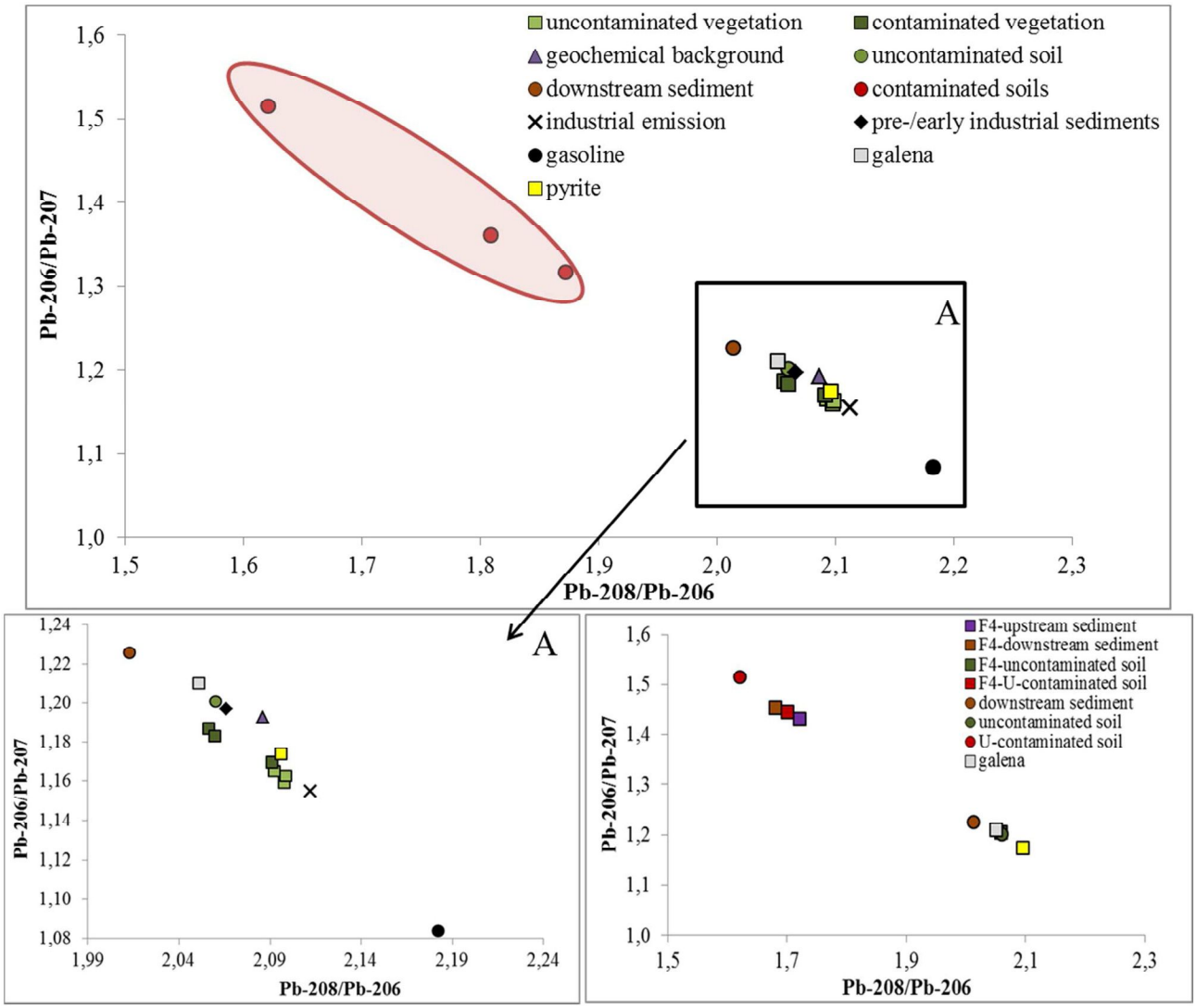

Fig. 3. Pb isotope ratios measured in bulk samples of the uncontaminated and the contaminated soils and sediments. Pb isotope ratios of vegetation samples and of the residual fraction (F4) from the sequential extraction are also reported. Data of industrial emission, pre/early industrial sediment and leaded gasoline are from Monna et al. (1997) and Véron et al. (1999). Data of galena and pyrite are from Lévêque (1990). Please note that the uncertainties of measurements are smaller than the symbols.

elements, depending on their nature, their speciation or the plant-species, including the case of mining contamination (Probst et al., 2009, Liu et al., 2005).

4.5. Identification of the potential sources of the contaminants

4.5.1. Using the Pb isotopes

In the uncontaminated soil, each fraction from sequential extraction has a specific Pb isotope signature. It indicates that the acid-soluble, the reducible, the oxidizable and the residual fractions release Pb from various origin. According to Bacon et al. (2006), anthropogenic Pb tends to be trapped in the two first mobile fractions of soils whereas Probst et al. (2003) identify organic matter and oxides as the main trapping compounds of atmospheric Pb derived from leaded gasoline combustion. In our study, the acid-soluble fraction of the uncontaminated soil or the upstream sediment does not exhibit Pb isotopic values typical of industrial emission or leaded gasoline (Monna et al., 1997, Véron et al., 1999). This suggests that contamination by atmospheric Pb remains negligible and that Pb mainly originates from soil minerals. However, the Pb isotope ratios of the vegetation sampled in the uncontaminated area, show inputs of anthropogenic Pb. According to Hernandez et al. (2003), one explanation could be that the Pb isotope ratios of the vegetation are reflective of the soil exchangeable fraction, which could have trapped exogenous Pb from past atmospheric inputs. In this way, the differences could be a result of the mixing of Pb signatures of different soil phases easy to desorb (water soluble, exchangeable and acid-soluble), all released in the operationally acid-soluble fraction. Atmospheric Pb is probably strongly retained in the topsoil (0–5 cm) without moving more deeply.

A Pb natural origin is also expected for the reducible and the oxidizable fractions of the reference soil and the upstream sediment. However, differences appear between the residual fractions of the two samples (Fig. 3). In the uncontaminated soil, the Pb isotope ratios of the residual fraction is close to the Bertholène galena ($^{206}Pb/^{207}Pb = 1.210$, $^{208}Pb/^{206}Pb = 2.051$) (Lévêque, 1990). The direct contribution from this mineral could explain the Pb isotope signature of the residual phase. On the contrary, the residual fraction of the upstream sediment shows radiogenic Pb isotope ratios. The low content in uranium and the radiological equilibria of the U-238 decay chain of this sediment exclude direct inputs of uranium mining contaminated material (Cuvier et al., 2015). The presence of natural U/Th bearing accessory resistant minerals, like monazite or zircon could explain the radiogenic Pb isotopes ratios of this fraction, since these mineral have been previously identified by SEM. The higher $^{208}Pb/^{206}Pb$ ratio of the residual fraction of the

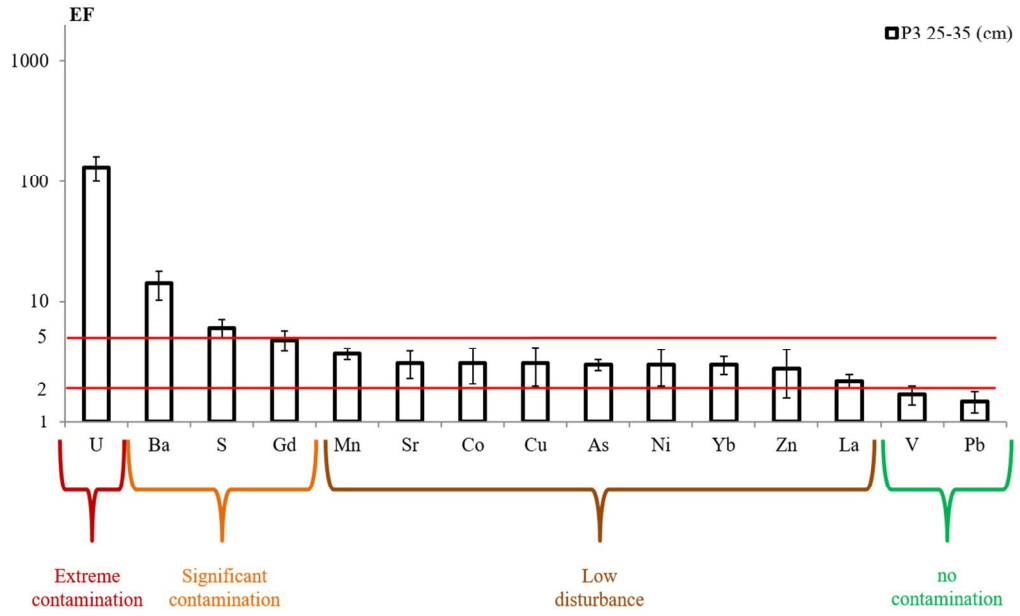

Fig. 4. Enrichment factor calculated for the contaminated soils (0–10 cm, n = 8) using P3(25–35) as reference material and Ti as reference element.

upstream sediment, compared to the total Pb signature of the contaminated soil, is consistent with this hypothesis. Finally, a natural origin, i.e. erosion of the uraniferous orthogneiss, is expected for the residue of the upstream sediment. However, past and actual operations realized in the Bertholène mine could have increased erosion of the surrounding rocks having a radiogenic Pb component. The erosion products would be then collected in the upstream part of the Balaures stream. Same explanation was previously invoked by Bollhöfer and Martin (2003) to explain radiogenic Pb signatures in surface scraped sediments in a catchment affected by U-mining activities in Australia.

High radiogenic ratios are measured in the total samples of contaminated soils. Inputs of radiogenic Pb from mining activities are the best way to explain the strong enrichment in ^{206}Pb and ^{207}Pb in respect to ^{208}Pb. Sediments contaminated by radiogenic material from U-mining activities exhibit an increase of the $^{206}Pb/^{207}Pb$ ratio only (Frostick et al., 2008). Santos and Tassinari (2012) found $^{206}Pb/^{207}Pb$ and $^{208}Pb/^{206}Pb$ ratios ranging from respectively 1.33 to 2.35 and from 0.991 to 1.905 in cores sampled in tailings located at a Portuguese uranium mine. In our study, the acid-soluble fraction of the contaminated soil records the highest radiogenic Pb ratio, confirming the exogenous and mining origin of these inputs, consistency with (1) the strong enrichments in U-238, Th-230 and Ra-226 and (2) the disequilibrium in the U-238 decay chain found in the contaminated area. The Pb isotope ratios of the residual fraction of the contaminated soil and the upstream sediment are relatively similar (Fig. 3). This could be a result of the presence of accessory minerals. However, the presence of others phases carrying radiogenic Pb and poorly extracted in the previous steps is not excluded. The fact that the residual fraction of the uncontaminated soil does not show this particular signature, suggests that the radiogenic minerals from weathering are transported by the Balaures stream from an upstream natural source, i.e. the Palanges orthogneiss, and not supply by the weathering of the underlying rock matter.

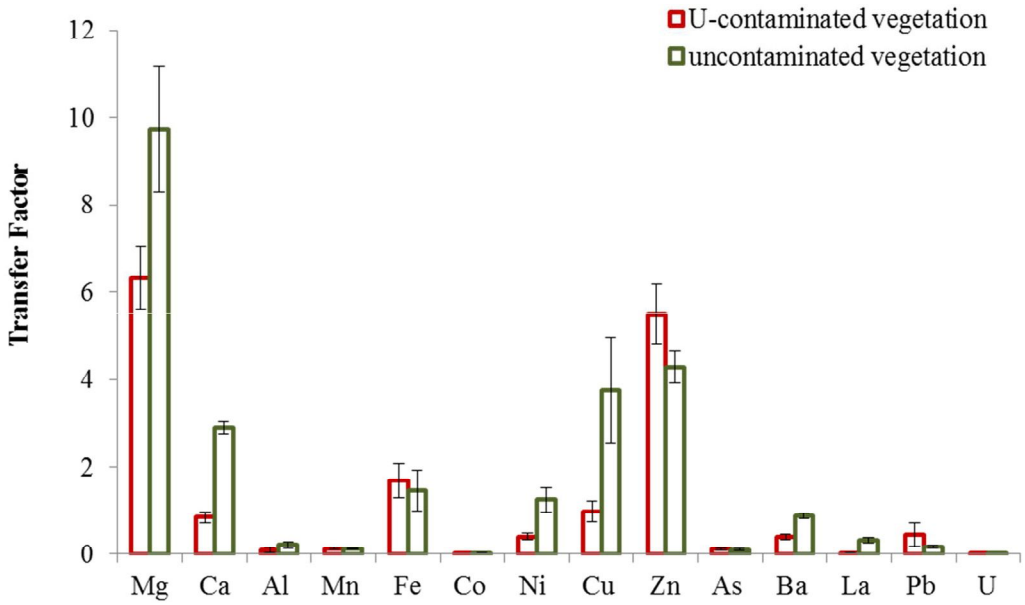

Fig. 5. Calculation of the transfer factor for both uncontaminated and contaminated plant samples based on the concentration of elements in the acid-soluble uncontaminated and contaminated soil fraction from sequential extraction.

Downstream sediment shows a $^{206}Pb/^{207}Pb$ ratio only slightly higher than the background value. Only one replicate of the residual fraction of the downstream sediment has radiogenic Pb ratios (Table 3). Scarce and specific phases like radiogenic accessory minerals probably contribute to the radiogenic signature of the residue but the presence of other phases having radiogenic Pb signatures can be assumed, since the $^{208}Pb/^{206}Pb$ ratio is significantly different from the upstream sediment and the contaminated soil. The downstream part of the Balaures stream does not exhibit sedimentation areas, implying that former sediments (in particular the fine fraction) were quickly re-mobilized and carried downstream. Sediments recently sampled probably do not show the same characteristic as former sediments, due to the mine closure and the mine releases processes. On the contrary, soils located in the radionuclide contaminated area must have retained influence from the mine. This assumption can explain the Pb isotope ratio differences between the contaminated soil and the downstream sediment.

The plot of total soil data in a $^{206}Pb/^{207}Pb$ in function of Ti/Pb diagram shows a significant linear correlation between the contaminated soil samples ($r = -0.97$, $R^2 = 0.94$, $p = 0.001$, $n = 6$) (see Supplementary Information SI-6). A binary mixing model can be inferred. The two endmembers are represented by the geochemical background and a radiogenic endmember from uranium mining, respectively. A $^{206}Pb/^{207}Pb$ isotopic ratio value of 2.263 can therefore be deduced for the radiogenic endmember. Assuming a two component mixing, the percentage of radiogenic Pb from uranium mining in the contaminated soil, calculated from (1), is around 26%. Using the same equation, the percentages of radiogenic Pb from uranium mining in each sequential leachates (F1, F2 and F3) of the contaminated soil are respectively 32%, 30% and 29%.

$$\text{Pb radiogenic } (\%) = \frac{\frac{206Pb}{207Pb}\,\text{sample} - \frac{206Pb}{207Pb}\,\text{background}}{\frac{206Pb}{207Pb}\,\text{radiogenic} - \frac{206Pb}{207Pb}\,\text{background}} \times 100 \quad (1)$$

Finally Pb isotope ratios and more particularly the $^{206}Pb/^{207}Pb$ one highlight four potential Pb sources measured in soils, sediments and vegetation: (1) the geochemical background measured in the uncontaminated soil, the contaminated vegetation and the downstream sediment, (2) the industrial emissions or leaded gasoline measured in the uncontaminated vegetation, (3) the releases from uranium mining processes (ore and wastes), which are the sources of exogenous radiogenic and mobile Pb measured in the acid-soluble fractions of the contaminated soils and finally (4) a probable mixture between natural radiogenic background due to the presence of accessory minerals and mining activities, which is the source of the immobile radiogenic Pb measured only in the residual fraction of the two sediments and contaminated soil.

4.5.2. Using the enrichment factors and the sequential extractions

In the contaminated samples, high Pearson correlation coefficients are found between EFs of S and Ba ($r = 0.99$, $R^2 = 0.986$, $p < 0.05$, $n = 20$). Considering the Ti-normalized data, a significant correlation is also found between EF of Ba and EF of Sr ($r = 0.99$, $R^2 = 0.99$, $p < 0.05$, $n = 20$) and between EF of S and EF of Sr ($r = 0.98$, $R^2 = 0.97$, $p < 0.05$, $n = 20$). This can be explained by the presence of barium sulfate in all contaminated soils and potentially linked to the U-mining activities. EDS probe analyses confirm the presence of Sr in the barite mineral.

Strong correlations are also found between EF of U and EF of REE, V, As, Co, Cu and Ni in the contaminated samples ($r = 0.83$–0.98, $R^2 = 0.69$–0.96, $p < 0.01$, $n = 10$). Such correlations can highlight similar chemical behavior, similar bearing phases, or similar sources. In the case of REE, the similar physical-chemistry properties of lanthanides and uranium explain the correlations (Aubert et al., 2004). Moreover the sequential extractions reveal that those elements, such as Co and Ni, are trapped in the same sequential fractions than uranium. On the contrary, V and As have different properties than U and are essentially located in the residual fraction. The correlations between EF of U and EFs of V and As could be explained in this case by a common origin of these three elements, i.e. from uranium bearing minerals and sulfide minerals from mining ore. Moreover, uranium vanadate minerals such as carnotite are found in the Bertholène uranium ore (Schmitt and Thiry, 1987). Finally, according to the correlation between the elements and considering the Pb isotope ratios of the contaminated samples, a mining origin is also expected for V, As, Co, Ni, Cu, Zn and REE. In both cases, the Balaures stream is the main vector of trace elements. The hypothesis of regular inputs from an upstream source, i.e. the mining site, to the downstream sediment is further supported by the observed high concentration of trace elements in the acid-soluble fraction. As a whole, the potential availability of trace elements is higher in the downstream sediment than in the contaminated soils, favoring their possible remobilization and their preferential trapping in the reducible fraction of soils, carried by Al- and Fe-oxides.

5. Conclusion

The purpose of this study was the evaluation of the contamination in trace elements associated with high uranium activity, downstream of a former French uranium mine. The level of contamination remains low ($2 < EF < 5$) except for U, S and Ba. However, the sequential extractions highlight modifications of the distribution of Ni, Co, Cu, Mn, Zn, U and REE, in the contaminated soils and sediments. Among the operationally-defined fractions of the standardized 3-step BCR procedure, the reducible fraction is pointed out as a major trace metal carrier.

Contaminated soils show a drastic shift to a radiogenic signature in Pb isotope ratios. As for the other contaminants, the acid-soluble and the reducible fractions show the largest radiogenic signals, involving a preferential trapping of mining radiogenic Pb. The residual fractions of the contaminated soil, the upstream sediment and, possibly, the downstream sediment, show an increase of radiogenic Pb, probably partially associated with natural radiogenic accessory minerals like monazite or zircon (containing also ^{208}Pb derived from thorium) carried by the Balaures stream. Inputs of immobile radiogenic Pb from mining activities could also be expected.

The linear correlation between the enrichment factor of trace elements can be the result of similar behavior and bearing phases. However, a common origin of those elements, i.e. the uranium ore and associated sulfide minerals, can also explain the correlation between trace elements having different properties or carried phases like V and As. The different geochemical tools used in this study underline that soils from the studied flooding surface have recorded and preserved the direct mining influence. On the contrary, the geochemical characteristics of downstream sediment have changed since the mine closure. The lack of sedimentation areas in the downstream part of the Balaures stream has favored the re-mobilization and the transportation of former fine sediments and prevented the conservation of the mining influence.

Finally, no striking modification of the transfer factor of trace elements from soil to stems and leaves appears at first sight. However, a future work will be required in order to perform a detailed study on the contaminant transfer from soil to roots and the further translocation to stems and leaves.

Acknowledgements

The authors would like to thank the technicians and engineers of the different analytical platforms used for this work (clean rooms, ICP-OES and ICP-MS, SEM and XRD at Observatoire Midi Pyrénées). They also wish the two anonymous reviewers for providing useful comments. This research was funded by a grant from the Région Midi-Pyrénées and IRSN.

Appendix A. Supplementary data

Supplementary data to this article can be found online at http://dx.doi.org/10.1016/j.scitotenv.2016.04.213.

References

Aubert, D., Probst, A., Stille, P., 2004. Distribution and origin of major and trace elements (particularly REE, U and Th) into labile and residual phases in an acid soil profile (Vosges Mountains, France). Appl. Geochem. 19 (6), 899–916. http://dx.doi.org/10.1016/j.apgeochem.2003.11.005.

Bäckström, M., Karlsson, S., Allard, B., 2004. Metal leachability and anthropogenic signal in roadside soils estimated from sequential extraction and stable lead isotopes. Environ. Monit. Assess. 90 (1–3), 135–160. http://dx.doi.org/10.1023/B:EMAS.0000003572.40515.31.

Bacon, J.R., Farmer, J.G., Dunn, S.M., Graham, M.C., Vinogradoff, S.I., 2006. Sequential extraction combined with isotope analysis as a tool for the investigation of lead mobilisation in soils: application to organic-rich soils in an upland catchment in Scotland. Environ. Pollut. 141 (3), 469–481. http://dx.doi.org/10.1016/j.envpol.2005.08.067.

Bartosiewicz, I., Chwastowska, J., Polkowska-Motrenko, H., 2015. Fractionation studies of trace elements in Polish uranium-bearing geological materials: potential environmental impact. Int. J. Environ. Anal. Chem. 95 (2), 121–134. http://dx.doi.org/10.1080/03067319.2014.994613.

Bermudez, G.M.A., Moreno, M., Invernizzi, R., Plá, R., Pignata, M.L., 2010. Evaluating top soil trace element pollution in the vicinity of a cement plant and a former opencast uranium mine in central Argentina. J. Soils Sediments 10 (7), 1308–1323. http://dx.doi.org/10.1007/s11368-010-0243-1.

Blaser, P., Zimmermann, S., Luster, J., Shotyk, W., 2000. Critical examination of trace element enrichments and depletions in soils: As, Cr, Cu, Ni, Pb, and Zn in Swiss forest soils. Sci. Total Environ. 249, 257–280.

Bollhöfer, A., and Martin, P. 2003. "Radioactive and radiogenic isotopes in Ngarradj (Swift Creek) sediments: a baseline study." Internal Report 404, February, Supervising Scientist, Darwin. Unpublished paper. http://cutlass.deh.gov.au/ssd/publications/ir/pubs/ir404.pdf.

Bollhöfer, A., Honeybun, R., Rosman, K., Martin, P., 2006. The lead isotopic composition of dust in the vicinity of a uranium mine in northern Australia and its use for radiation dose assessment. Sci. Total Environ. 366 (2–3), 579–589. http://dx.doi.org/10.1016/j.scitotenv.2005.11.016.

Bourennane, H., Douay, F., Sterckeman, T., Villanneau, E., Ciesielski, H., King, D., Baize, D., 2010. Mapping of anthropogenic trace elements inputs in agricultural topsoil from northern France using enrichment factors. Geoderma 157 (3–4), 165–174. http://dx.doi.org/10.1016/j.geoderma.2010.04.009.

Carlsson, E., Büchel, G., 2005. Screening of residual contamination at a former uranium heap leaching site, Thuringia, Germany. Chemie Der Erde – Geochem. 65 (September), 75–95. http://dx.doi.org/10.1016/j.chemer.2005.06.007.

Chester, R., Stoner, J.H., 1973. Pb in particulates from the lower atmosphere of the eastern Atlantic. Nature 245, 27–28.

Covelli, S., Fontolan, G., 1997. Application of a normalization procedure in determining regional geochemical baselines. Environ. Geol. 30 (1–2), 34–45.

Cuvier, A., 2015. Accumulation et sources de l'uranium, de ses descendants et des éléments traces métalliques dans les zones humides autour des anciens sites miniers uranifères. Thèse de doctorat de l'Institut National Polytechnique de Toulouse (376pp.).

Cuvier, A., Panza, F., Pourcelot, L., Foissard, B., Cagnat, X., Prunier, J., van Beek, P., Souhaut, M., Le Roux, G., 2015. Uranium decay daughters from isolated mines: accumulation and sources. J. Environ. Radioact. 149 (November), 110–120. http://dx.doi.org/10.1016/j.jenvrad.2015.07.008.

Davidson, C.M., Duncan, A.L., Litteljohn, D., Ure, A.M., Garden, L.M., 1998. A critical evaluation of the three stage BCR sequential extraction procedure to assess the potential mobility and toxicity of heavy metals in industrially-contaminated land. Anal. Chim. Acta 363, 45e55.

Dhoum, R.T., Evans, G.J., 1998. Evaluation of uranium and arsenic retention by soil from a low level radioactive waste management site using sequential extraction. Appl. Geochem. 13 (4), 415–420.

Ettler, V., Mihaljevič, M., Šebek, O., Molek, M., Grygar, T., Zeman, J., 2006. Geochemical and Pb isotopic evidence for sources and dispersal of metal contamination in stream sediments from the mining and smelting district of Příbram, Czech Republic. Environ. Pollut. 142 (3), 409–417. http://dx.doi.org/10.1016/j.envpol.2005.10.024.

Frostick, A., Bollhöfer, A., Parry, D., Munksgaard, N., Evans, K., 2008. Radioactive and radiogenic isotopes in sediments from Cooper Creek, western Arnhem Land. J. Environ. Radioact. 99 (3), 468–482. http://dx.doi.org/10.1016/j.jenvrad.2007.08.015.

Frostick, A., Bollhöfer, A., Parry, D., 2011. A study of radionuclides, metals and stable lead isotope ratios in sediments and soils in the vicinity of natural U-mineralisation areas in the Northern Territory. J. Environ. Radioact. 102 (10), 911–918. http://dx.doi.org/10.1016/j.jenvrad.2010.04.003.

Hernandez, L., Probst, A., Probst, J.-L., Ulrich, E., 2003. Heavy metal distribution in some French forest soils: evidence for atmospheric contamination. Sci. Total Environ. 312 (1), 195–219.

Hirner, A.V., 1992. Trace element speciation in soils and sediments using sequential chemical extraction methods. Int. J. Environ. Anal. Chem. 46 (1–3), 77–85. http://dx.doi.org/10.1080/03067319208026999.

Howe, S.E., Davidson, C.M., McCartney, M., 2002. Determination of uranium concentration and isotopic composition by means of ICP-MS in sequential extracts of sediment from the vicinity of a uranium enrichment plant. J. Anal. At. Spectrom. 17 (5), 497–501. http://dx.doi.org/10.1039/b200270c.

Humbert, J., 1986. Le Traitement Des Minerais D'uranium à Bertholène. Industrie Minérale, Mines et Carrières. Les Techniques 68 (9), 434–440.

Kipp, G., Stone, J.J., Stetler, L.D., 2009. Arsenic and uranium transport in sediments near abandoned uranium mines in Harding County, South Dakota. Appl. Geochem. 24 (12), 2246–2255. http://dx.doi.org/10.1016/j.apgeochem.2009.09.017.

Krachler, M., Le Roux, G., Kober, B., Shotyk, W., 2004. Optimising accuracy and precision of lead isotope measurement (^{206}Pb, ^{207}Pb, ^{208}Pb) in acid digests of peat with ICP-SMS using individual mass discrimination correction. J. Anal. At. Spectrom. 19 (3), 354. http://dx.doi.org/10.1039/b314956k.

Kyser, K., Lahusen, L., Drever, G., Dunn, C., Leduc, E. and Chipley, D. 2015. "Using Pb isotopes in surface media to distinguish anthropogenic sources from undercover uranium sources." Comptes Rendus Geosci. doi:http://dx.doi.org/10.1016/j.crte.2015.06.003 (Accessed September 8).

Larson, L.N., Stone, J.J., 2011. Sediment-bound arsenic and uranium within the Bowman–Haley Reservoir, North Dakota. Water Air Soil Pollut. 219 (1–4), 27–42. http://dx.doi.org/10.1007/s11270-010-0681-9.

Lévêque, M.-H., 1990. Contribution de La Géochronologie U-Pb à La Caractérisation Du Magmatisme Cadomien de La Partie Sud-Est Du Massif Central et Du Gisement D'uranium Associé de Bertholène. Montpellier 2 (http://www.theses.fr/1990MON20080).

Lévêque, M.H., Lancelot, J.R., George, E., 1988. The bertholene uranium deposit mineralogical characteristics and U-Pb dating of the primary U mineralization and its subsequent remobilization: consequences upon the evolution of the U deposits of the Massif Central. France. Chem. Geol. 69, 147–163.

Liu, H., Probst, A., Liao, B., 2005. Metal contamination of soils and crops affected by the Chenzhou lead/zinc mine spill (Hunan, China). Sci. Total Environ. 339 (1–3), 153–166. http://dx.doi.org/10.1016/j.scitotenv.2004.07.030.

Luoma, S.N., 1990. Processes affecting metal concentrations in estuarine and coastal marine sediments. Heavy Metals in Marine Environment. CRC Press, Boca Raton Fl, pp. 51–66.

Martin, R., Sanchez, D.M., Gutierrez, A.M., 1998. Sequential extraction of U, Th, Ce, La and some heavy metals in sediments from Ortigas River, Spain. Talanta 46 (5), 1115–1121.

Meca, S., Gimenez, J., Casas, I., Marti, V., de Pablo, J., 2012. Uranium speciation in river sediments contaminated by phosphates ores. Environ. Chem. Lett. 10, 49–53. http://dx.doi.org/10.1007/s10311-011-0327-1.

Monna, F., Lancelot, J., Croudace, I.W., Cundy, A.B., Lewis, J.T., 1997. Pb isotopic composition of airborne particulate material from France and the southern United Kingdom: implications for Pb pollution sources in urban areas. Environ. Sci. Technol. 31 (8), 2277–2286.

N'Guessan, Y.M., Probst, J.L., Bur, T., Probst, A., 2009. Trace elements in stream bed sediments from agricultural catchments (Gascogne Region, S-W France): where do they come from? Sci. Total Environ. 407 (8), 2939–2952. http://dx.doi.org/10.1016/j.scitotenv.2008.12.047.

Noller, B.N., 1991. Non-radiological contaminants from uranium mining and milling at Ranger, Jabiru, Northern Territory, Australia. Environ. Monit. Assess. 19 (1–3), 383–400. http://dx.doi.org/10.1007/BF00401327.

Probst, A., Hernandez, L., Probst, J.L., 2003. Heavy metals partioning in three French forest soils by sequential extraction procedure. J. de Physique IV – Proc. 107, 4. http://dx.doi.org/10.1051/jp4:20030493.

Probst, A., Liu, H., Fanjul, M., Liao, B., Hollande, E., 2009. Response of *Vicia faba* L. to metal toxicity on mine tailing substrate: geochemical and morphological changes in leaf and root. Environ. Exp. Bot. 66 (2), 297–308. http://dx.doi.org/10.1016/j.envexpbot.2009.02.003.

Quevauviller, P., Rauret, G., Muntau, H., Ure, A.M., Rubio, R., Lopez Sanchez, J.F., et al., 1994. Evaluation of a sequential extraction procedure for the determination of extractable trace metal contents in sediments. Fresenius J. Anal. Chem. 349, 808–814.

Rao, C.R.M., Sahuquillo, A., Lopez-Sanchez, J.-F., 2010. Comparison of single and sequential extraction procedures for the study of rare earth elements remobilisation in different types of soils. Anal. Chim. Acta 662 (2), 128–136. http://dx.doi.org/10.1016/j.aca.2010.01.006.

Rauret, G., 1998. Extraction procedures for the determination of heavy metals in contaminated soil and sediment. Talanta 46 (3), 449–455. http://dx.doi.org/10.1016/S0039-9140(97)00406-2.

Rauret, G., Lopez-Sanchez, J.-F., Sahuquillo, A., Rubio, R., Davidson, C., Ure, A., Quevauviller, P., 1999. Improvement of the BCR three step sequential extraction procedure prior to the certification of new sediment and soil reference materials. J. Environ. Monit. 1 (1), 57–61.

Reimann, C., de Caritat, P., 2005. Distinguishing between natural and anthropogenic sources for elements in the environment: regional geochemical surveys versus enrichment factors. Sci. Total Environ. 337 (1–3), 91–107. http://dx.doi.org/10.1016/j.scitotenv.2004.06.011.

Santos, R.M.P., Tassinari, C.C.G., 2012. Different lead sources in an abandoned uranium mine (Urgeirica - Central Portugal) and its environment impact - isotopic evidence. Geochem.: Explor., Environ., Anal. 12 (3), 241–252. http://dx.doi.org/10.1144/1467-7873/11-RA-076.

Schiff, K.C., Weisberg, S.B., 1999. Iron as a reference element for determining trace metal enrichment in southern California coastal shelf sediments. Mar. Environ. Res. 48 (2), 161–176.

Schmitt, J.M., Baubron, J.C., Bonhomme, M.G., 1984. Pétrographie et Datations K-Ar Des Transformations Minérales Affectant Le Gîte Uranifère de Bertholène (Aveyron—France). Mineral. Deposita 19 (2), 123–131.

Schmitt, J.M., Thiry, M., 1987. Uranium behaviour in a Gossan-Type weathering system: example of the bertholene deposit (Aveyron, France). http://inis.iaea.org/Search/search.aspx?orig_q=RN:18085068.

Sen, I.S., Peucker-Ehrenbrink, S., 2012. Anthropogenic disturbance of element cycles at the earth's surface. Environ. Sci. Technol. 46 (16), 8601–8609. http://dx.doi.org/10.1021/es301261x.

Skipperud, L., Strømman, G., Yunusov, M., Stegnar, P., Uralbekov, B., Tilloboev, H., Zjazjev, G., Heier, L.S., Rosseland, B.O., Salbu, B., 2013. Environmental impact assessment of radionuclide and metal contamination at the former U sites Taboshar and Digmai, Tajikistan. J. Environ. Radioact. 123 (September), 50–62. http://dx.doi.org/10.1016/j.jenvrad.2012.05.007.

Smodiš, B., Štrok, M., Černe, M., 2012. Radioecology studies in the vicinity of a closed uranium mine. EPJ Web of Conferences Vol. 24: 06008. http://dx.doi.org/10.1051/epjconf/20122406008.

Steinmann, M., Stille, P., 1997. Rare earth element behavior and Pb, Sr, Nd isotope systematics in a heavy metal contaminated soil. Appl. Geochem. 12 (5), 607–623. http://dx.doi.org/10.1016/S0883-2927(97)00017-6.

Štrok, M., Smodiš, B., 2013. Partitioning of natural radionuclides in sediments around a former uranium mine and mill. J. Radioanal. Nucl. Chem. 297 (2), 201–207. http://dx.doi.org/10.1007/s10967-012-2364-z.

Thompson, P.A., Kurias, J., Mihok, S., 2005. Derivation and use of sediment quality guidelines for ecological risk assessment of metals and radionuclides released to the environment from uranium mining and milling activities in Canada. Environ. Monit. Assess. 110 (1–3), 71–85. http://dx.doi.org/10.1007/s10661-005-6291-0.

Véron, A., Flament, P., Bertho, M.-L., Alleman, L., Flegal, R., Hamelin, B., 1999. Isotopic evidence of pollutant lead sources in northwestern France. Atmos. Environ. 33 (20), 3377–3388. http://dx.doi.org/10.1016/S1352-2310(98)00376-8.

Wedepohl, K.H., 1995. The composition of the continental crust. Geochim. Cosmochim. Acta 59 (9), 1217–1232.

Whalley, C., Grant, A., 1994. Assessment of the phase selectivity of the European Community Bureau of Reference (BCR) sequential extraction procedure for metals in sediment. Anal. Chim. Acta 291 (3), 287–295.

Windom, H.L., Schropp, S.J., Calder, F.D., Ryan, J.D., Smith Jr., R.G., Burney, L.C., Lewis, F.G., Rawlinson, C.H., 1989. Natural trace metal concentrations in estuarine and coastal marine sediments of the southeastern United States. Environ. Sci. Technol. 23 (3), 314–320.

Yeghicheyan, D., Bossy, C., Le Coz, M.B., Douchet, C., Granier, G., Heimburger, A., Lacan, F., et al., 2013. A compilation of silicon, rare earth element and twenty-one other trace element concentrations in the natural river water reference material SLRS-5 (NRC-CNRC). Geostand. Geoanal. Res. 37 (4), 449–467. http://dx.doi.org/10.1111/j.1751-908X.2013.00232.x.